Friction **10**(12): 2069–2085 (2022)
https://doi.org/10.1007/s40544-021-0578-1
ISSN 2223-7690
CN 10-1237/TH

RESEARCH ARTICLE

Tribological performance of iron- and nickel-base self-lubricating claddings containing metal sulfides at high temperature

Hector TORRES[1,2,*], Tugce CAYKARA[2], Jens HARDELL[2], Janne NURMINEN[3], Braham PRAKASH[2,4], Manel RODRÍGUEZ RIPOLL[1]

[1] *AC2T research GmbH, Viktor-Kaplan-Straße 2/C, Wiener Neustadt 2700, Austria*

[2] *Department of Applied Physics and Mechanical Engineering, Luleå University of Technology, Luleå 97187, Sweden*

[3] *Castolin Eutectic GmbH, Gutenbergstraße 10, Kriftel 65830, Germany*

[4] *Department of Mechanical Engineering, Tsinghua University, Beijing 100084, China*

Received: 30 December 2020 / Revised: 30 March 2021 / Accepted: 01 December 2021

Abstract: Iron-based coatings with the incorporation of solid lubricants have been prepared by means of laser cladding, in an effort to control friction and decrease tool wear at high temperatures during metal forming applications. The choice of a Fe-based powder has been considered advantageous, as it can lead to decreased costs compared to nickel-based claddings previously studied by the authors, in addition to having a lower environmental impact. In particular, the incorporation of transition metal dichalcogenides such as MoS_2 as precursors leads to the encapsulation of silver in Fe-based self-lubricating claddings, resulting in a uniform distribution of the soft metal across the thickness of the coating. Subsequent tribological evaluation of the claddings at high temperatures shows that the addition of lubricious compounds leads to lower friction at room temperature and significantly decreased wear up to 600 °C compared to the unmodified iron-based reference alloy, although higher than similar self-lubricating Ni-based claddings. In order to cast light into these observed differences, the corresponding microstructures, phase composition, and self-lubricating mechanisms have been studied and compared for Fe- and Ni-based claddings having both of them the addition of silver and MoS_2. The results suggest a key role of the formation of protective tribolayers on the counter body during high temperature sliding contact. Additional simulation of the phase evolution during solidification reveals that the formation of different chromium- and nickel-based metal sulfides in Fe- and Ni-claddings during laser cladding by the decomposition of MoS_2 plays a key role in determining their tribological behaviour at high temperatures.

Keywords: high temperature; laser cladding; self-lubrication; metal forming; chromium sulphide; MoS_2

1 Introduction

Self-lubricating coatings capable of decreasing friction and wear at high temperatures (HT) have been the subject of significant interest since the 1970s in applications including aerospace, metal forming, or power generation, to name a few. In such processes, temperatures above 350 °C lead to the quick thermal degradation of conventional lubricants like oils and greases, necessitating the use of new lubrication approaches based on solid lubricants capable of providing low and stable friction at HT [1–6]. The incorporation of solid lubricants in HT coatings has been the subject of significant interest since the pioneering work of Sliney [7], with similar approaches reported in the available literatures for thin-film physical vapor deposition (PVD) coatings [8–11], plasma spray [12], or bulk materials prepared by means

* Corresponding author: Hector TORRES, E-mail: hector.torres@ac2t.at

of powder sintering [13–16].

Laser cladding is a well-known coating preparation technique which has been extensively used in recent years for the deposition of thick protective coatings, allowing in particular the repair and re-working of high-value industrial components. This deposition technique has also significant advantages like the low defect density of the resulting coatings [17], their excellent metallurgical bonding with the substrate [18], and the low heat-affected zone (HAZ) on the substrate [19, 20]. For these reasons, laser cladding has become widespread for applications such as the automotive [21] or for the repair of turbine blades [22]. In recent years, self-lubricating laser claddings have been described in the available literatures [23–27], including silver, copper, transition metal dichalcogenides (TMDs) such as MoS_2 and WS_2, and alkaline-earth fluorides such as CaF_2, by mixing the solid lubricants mechanically with the base powder used for the cladding preparation. Further, the thermal degradation of solid lubricants such as MoS_2 or WS_2 during the cladding process has also been described in the literature. In particular, Yang et al. [26] prepared NiCr–Cr_3C_2 laser claddings with the addition of 30 wt% WS_2 as a solid lubricant, leading to decreased friction and wear up to 300 °C compared to the unmodified alloy, attributed to the formation of lubricant patches made of a mixture of WS_2 with chromium sulfides forming from the thermal degradation of TMDs during laser cladding. Similar results have been reported in the context of Ni-based laser claddings with the incorporation of MoS_2 by Niu et al. [25] in addition to Xu et al. [28].

In a similar fashion, Torres et al. reported the formation of chromium sulfides due to the thermal degradation of both MoS_2 and WS_2 added to NiCrSiB-based laser claddings [23], with the resulting self-lubricating coatings showing decreased friction up to temperatures of 600 °C. From the previous, it can be assumed that chromium-based sulfides can provide effective HT lubrication, even if the underlying mechanisms are not yet completely understood. Although the literature gives proof of self-lubricating claddings with a good tribological behaviour at HT, it is interesting to note here that the coatings described in the available literature are overwhelmingly nickel-based. This has been attributed to the lower melting point of self-fluxing Ni-mixtures featuring the addition of Si and B [29], which makes cladding preparation easier. On the other hand, only a few iron-based self-lubricating claddings have been studied very recently in the available literatures [30, 31], even though such claddings would lead to decreased costs while being less environmentally harmful than their nickel-based counterparts. Another interesting fact is that most of the available literatures on the tribology at HT of self-lubricating materials report the use of non-metallic counter bodies such as Al_2O_3 or Si_3N_4, which are not representative of metal forming processes. While OuYang et al. did study Fe-based self-lubricating claddings with the incorporation of WS_2 as a solid lubricant and evaluated their tribological behaviour at HT, a ceramic counter body of Si_3N_4 was chosen [32]. In fact, the use of metallic counter bodies is still underrepresented in the available literatures, restricted mostly to room temperature testing [33, 34]. The investigation of the tribological behaviour of steel-based counter bodies sliding against self-lubricating laser claddings at high temperature is an important step towards understanding the friction and wear behaviour under more representative conditions.

In order to bridge these perceived research gaps, the novelty of this work lies in addressing the following points:

1) Development of a set of iron-based laser claddings with and without the addition of solid lubricants for prospective HT applications.

2) Investigation of the tribological performance of the self-lubricating claddings under conditions representative of metal forming applications such as the hot stamping of ultra-high strength steel. For this reason, the use of ceramic counter bodies has been avoided, as they can lead to very different tribological behaviour compared to metal-based ones [35].

3) Comparison of the HT self-lubricating performance of the developed Fe-based claddings against nickel-based self-lubricating claddings reported in previous studies by the authors.

4) Identification of the lubrication mechanism.

The role of compounds such as chromium- or nickel sulfides in terms of their tribological behaviour is far from being understood. To shed some light into the issue, the phase evolution during solidification of both iron- and nickel-based claddings has been

simulated by means of Thermocalc software, and compared with the results obtained by characterisation techniques such as electron backscatter diffraction (EBSD) on the as-deposited claddings. This information is expected to identify the compounds providing effective lubrication at HT.

It is expected that the present study can cast further light into the potential of Fe-based self-lubricating claddings in HT applications, in addition to understand more in-depth the microstructural evolution and phase content of TMD-containing claddings.

2 Experimental

2.1 Materials

For the present study, different iron-based coatings were deposited by means of laser cladding using a direct diode laser system on AISI 304 stainless steel plates. The base powder had a chromium content as high as 17 wt%, expected to improve oxidation resistance at HT, with its full chemical composition being summarised in Table 1. The corresponding particle size ranged from 45 to 106 μm. Interestingly, in the present study, small amounts of Mn could be detected in the as-deposited Fe-based claddings, which could be due to dilution from the stainless steel substrate during melting with the laser.

Silver and MoS_2 were chosen as the solid lubricants to be incorporated in the self-lubricating claddings. It must be noted here that silver is a soft metal capable of forming an easy-to-shear layer in the contact surface decreasing friction [36]. MoS_2 belongs to a class of lamellar metal sulfides (TMDs) with weak van der Waals bonding between sulfur atoms, leading to easy shearing and thus improved tribological behaviour [37, 38].

For the cladding deposition process, the base powder was mechanically mixed with fixed wt% concentrations of the aforementioned solid lubricants using ethanol as the binder, and the resulting paste was spread on stainless steel substrates. Ag powder was procured from Goodfellow, with a maximum particle size of 45 μm while MoS_2 powder with a size between 5 and 75 μm was provided by Tribotecc GmbH.

After drying for 1 h at 100 °C in a furnace, single-pass laser cladding was performed under an argon protective atmosphere using rectangular shaped beams of 24 mm × 3 mm and 24 mm × 6 mm. Power densities and energy inputs for the Fe-based were in the 40 to 50 W/mm² and 6 to 8 J/mm³ ranges. Further detail on the deposition process for the Ni-based claddings is given in a previous paper by the authors [24].

The content of solid lubricants for each laser cladding is summarised in Table 2. For Ni–5Ag–10MoS_2, 5 wt% Ag and 10 wt% MoS_2 were added to the powder mixture as this composition was found in a previous study by the authors to lead to an optimum microstructure in terms of solid lubricants distribution across the coating [24]. An iron-based self-lubricating cladding was also prepared for the present study, Fe–5Ag–10MoS_2, featuring 5 wt% silver and 10 wt% MoS_2. Additionally, a reference Fe-based cladding without the addition of any solid lubricant was also prepared for comparison with the self-lubricating claddings previously described. As seen in Table 2, both Fe-based claddings were harder than their nickel-based counterpart due to their martensitic microstructure, as shown in Fig. 1(c).

Sample preparation prior to testing for all of the samples included the manual grinding using #360 and #600 SiC abrasive paper, rotating the sample during the last step to prevent any directionality of the resulting surface lay. The roughness Ra was measured prior to testing using a Zygo New View 7300 3D optical profiler.

The counter body samples for this study were manufactured from AISI 52100 bearing steel, with an

Table 1 Chemical composition (wt%) of the base powders used for the preparation of the laser claddings.

	C	Cr	Si	B	Fe	Ni
Fe-based	0.18	17	—	—	Balance	1
Ni-based	0.2	4	2.5	1	< 2	Balance

Table 2 Solid lubricant content for the tested materials.

Material	Solid lubricant content (wt%)		RT hardness (HV10)	Ra (μm)
	Ag	MoS_2		
Fe–5Ag–10MoS_2	5	10	542 ± 30	0.18 ± 0.06
Fe–Reference	0	0	535 ± 6	0.07 ± 0.02
Ni–5Ag–10MoS_2	5	10	398 ± 5	0.10 ± 0.03

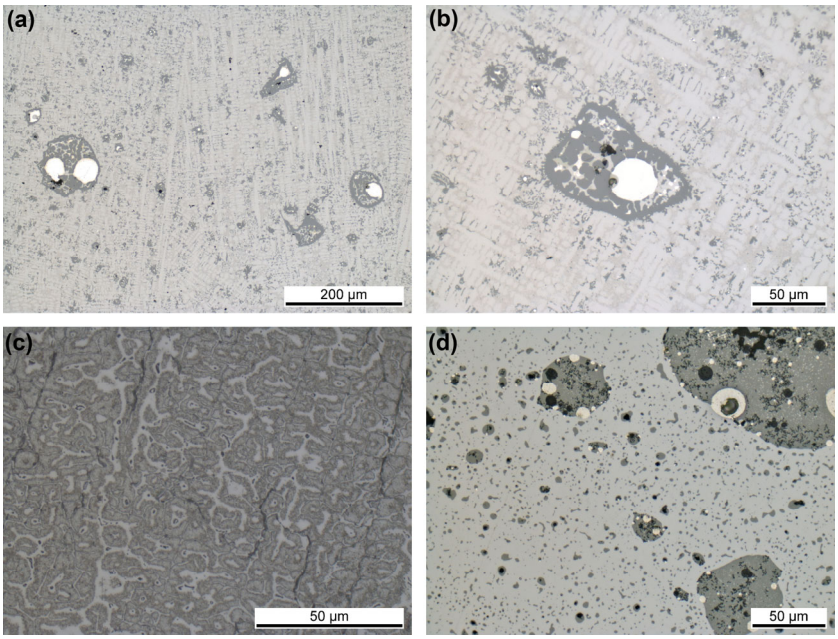

Fig. 1 Optical microscopy of the as-deposited self-lubricating claddings. (a) Ni–5Ag–10MoS_2 with (b) a detail thereof, in addition to (c) the reference Fe-based alloy, chemically etched to highlight the martensitic microstructure and (d) Fe–5Ag–10 MoS_2.

as-delivered hardness measured to be 873 ± 19 HV10 [39]. All the specimens used for the HT reciprocating tests were ultrasonically cleaned in industrial heptane and rinsed with acetone before and after testing.

2.2 High temperature reciprocating tests

For this series of tests, the tribological behaviour of the claddings was studied using an Optimol SRV friction and wear tester, which is described in further detail in Ref. [23]. The upper counter body samples were pins with a diameter of 2 mm machined from AISI 52100 bearing steel needle rollers, representing in this case a low alloy steel workpiece material in a hot forming process. The pin samples were loaded against a stationary flat sample using a spring deflection mechanism and subsequently oscillated by means of an electromagnetic drive.

The laser claddings were subsequently tested at RT, 400, and 600 °C. Heating of the lower samples was accomplished using the integrated resistive heater in the lower specimen holder, with sample surface temperatures being measured using a thermocouple prior to test start in order to provide an accurate temperature estimate.

The cladding samples were machined to a size of 12.6 mm × 12.6 mm × 4.7 mm. Reciprocating frequency and stroke length were adjusted to 13 Hz and 4 mm respectively so that the average sliding speed for all of the tests was 0.1 m/s while the applied load was set to 50 N, in order to reach a contact pressure of 16 MPa. These values were chosen as they were close to the ones quoted in the literature for hot sheet metal forming [40–45]. The test duration was set to 900 s, leading to a total sliding distance of 90 m, and in order to ensure repeatability three repetitions were performed for each condition. The testing parameters are summarised in Table 3.

2.3 Surface and microstructure characterisation

Characterisation of the as-deposited claddings in addition to tested samples, including measurements of their chemical composition by means of energy-dispersive X-ray spectroscopy (EDS), was performed

Table 3 Test parameters chosen for the HT reciprocating tests against AISI 52100 flat pins.

Load (N)	50
Cladding sample temperatures (°C)	RT, 400, 600
Reciprocating frequency (Hz)	13
Stroke length (mm)	4
Duration (s)	900

by means of a JSM-IT300 scanning electron microscope (SEM).

Electron backscatter diffraction (EBSD) has also been used for the characterisation of both as-deposited coatings. In the present study, a JEOL JIB-4700F Multi Beam System equipped with an e-Flash EBSD system have been used. Mapping was performed on an area of 8.5 μm × 6.5 μm for the iron-based cladding with a 20 kV acceleration voltage. Patterns were acquired with an acquisition time of 30 ms.

2.4 Phase diagram calculations

Phase diagram calculations were performed using Thermocalc. This is a phase calculation software based on thermodynamical principles, with abundant applications in metallurgy processes involving melting and solidification. It must be reminded here that the calculations can predict phases in thermodynamic equilibrium; fast cooling after laser cladding processes may prevent the formation of predicted phases or lead to the precipitation of different, metastable compounds.

For the present calculations it has been assumed that MoS_2 completely decomposes in the melt pool due to the very high temperature. Silver, the other solid lubricant incorporated to the claddings, could not be added to the simulation as it was not included in the available database. Additionally, a Mn content of 1 wt% was included for the iron-based system, as EDS measurements performed on the as-deposited Fe–5Ag–10MoS_2 were able to detect a small amount of Mn, possibly due to dilution from the AISI 304 substrate.

The chemical composition for both systems to be simulated was chosen as follows: for NiCrSiB–MoS_2, 79 wt% Ni, 4 wt% Cr, 2.5 wt% Si, 1.0 wt% B, 0.5 wt% C, 10 wt% Mo, and 3 wt% S. while for FeCrNi–MoS_2, it was 70.82 wt% Fe, 17.0 wt% Cr, 1.0 wt% Ni, 0.18 wt% C, 1 wt% Mn, and 10 wt% MoS_2.

3 Results and discussion

3.1 Microstructure of the self-lubricating claddings

The microstructures of the resulting iron- and nickel-based claddings are shown in Figs. 1(a) and 1(b). The presence of a dark phase across the thickness of the coating could be seen for both self-lubricating claddings, with bright particles observed in both cases in connection with it.

Further characterisation was performed on the as-deposited Fe–5Ag–10MoS_2 by means of SEM/EDS (Fig. 2). The brighter phase (spot A in Table 4) was comprised of silver particles, while the dark phase previously described (spot B in Table 4) are Cr- and S-rich and had a chemical composition consistent with chromium sulfides, compounds formed due to the thermal degradation of MoS_2 and other transition metal dichalcogenides taking place during laser cladding, which are known to be effective solid lubricants at HT [46, 47]. In a previous study by the authors, this phase has been shown to be a mixture of chromium sulfides [48]. It has also been found that the sulfide-rich phase was able to encapsulate the silver phase, forming aggregates occasionally as large as 100 μm. Spot C in Table 4 corresponds to the hardfacing matrix, which was observed to have a 10 at% contents of Cr compared to the original 17 at%. This suggests a depletion of chromium from the

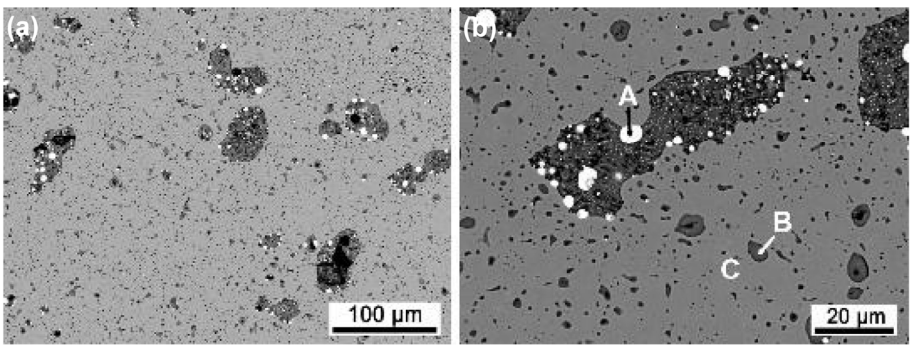

Fig. 2 (a) SEM overview performed on a cross section of the Fe–5Ag–10MoS_2 self-lubricating cladding, with (b) a detailed view of one of the aggregates found in the coating microstructure.

Table 4 Composition as measured by EDS of the spots marked in Fig. 2(b).

Spot	Chemical composition (at%)						
	Fe	Ni	Mo	Cr	S	Si	Ag
A	—	—	—	—	—	—	100.0
B	6.0	—	—	54.8	37.4	—	1.9
C	83.9	1.6	4.5	10.0	—	0.8	—

matrix leading to the formation of chromium sulfides during laser cladding. The microstructure of Ni–5Ag–10MoS_2 is described in further detail in a previous study by the authors [46].

The results of the EBSD measurements performed on the as-deposited nickel-based Ni–5Ag–10MoS_2 self-lubricating cladding are summarised in Fig. 3, with phase contents listed in Table 5. Due to its similar crystallographic structure to the face-centered cubic (fcc) nickel matrix, silver could not be quantified. In particular, the dark aggregates seen in Fig. 1(b) were found to consist of a mixture of chromium sulfides such as CrS and Cr_3S_4, with a joint phase content as high as 18%. Additionally, the formation of nickel sulfides such as NiS_2 could be attested by means of EBSD, with a lower phase content of 6.6%. This appears to be in accordance with the available literature suggesting that Cr-based sulfides are thermodynamically more stable than their Ni-based counterparts [50]. Also interestingly, a small fraction of MoS_2 could also be detected, which raised the possibility that it did not thermally decompose during the cladding process, although it is also possible that it re-formed during sample cooling.

Similar measurements performed on the as-deposited Fe–5Ag–10MoS_2 are summarised in Fig. 4 and Table 5. In this case, the cladding matrix consisted as expected mostly of martensite, with some retained austenite.

Table 5 Phase content, as measured by EBSD, for Ni–5Ag–10MoS_2 and Fe–5Ag–10MoS_2.

Ni–5Ag–10MoS_2		Fe–5Ag–10MoS_2	
Phase	(%)	Phase	(%)
Ni (fcc)	71.4	Iron (martensite)	84.5
CrS	8.2	Iron (austenite)	3.7
Cr_3S_4	10.6	CrS	10.9
NiS_2	6.6	Cr_2S_3	0.8
MoS_2	3.2	MoS_2	0.2

The sulfide aggregates seen in Fig. 2 were found to consist of a mixture of chromium sulfides, mainly CrS with a smaller contribution of Cr_2S_3. As in the case of the nickel based self-lubricating cladding, some small amount of MoS_2 could be found after the laser melting process, although in lower concentrations, with no evident explanation for this fact. Other sulfide compounds such as FeS and FeS_2 could not be detected by means of EBSD, and spot B in Table 4 is considered to be chromium sulfide with a small iron contribution measured from the surrounding martensitic matrix.

Phase diagram simulations of the solidification process for both self-lubricating claddings using Thermocalc are summarised in Fig. 5. For the system NiCrSiB–10MoS_2, it can be seen that the melt pool consisted of two different liquid phases, as seen in the nickel-sulfur binary phase diagrams [51]. Solidification was predicted to start at ~1,300 °C with the formation of a fcc nickel-based matrix and chromium borides (labelled as MB_B33), co-existing with a liquid phase down to ~900 °C. Temperatures lower than 1,250 °C were in turn required for the precipitation of metallic sulfides, in stark contrast to other simulations performed in Ni-based claddings predicting their formation at temperatures as high as 3,000 °C [52].

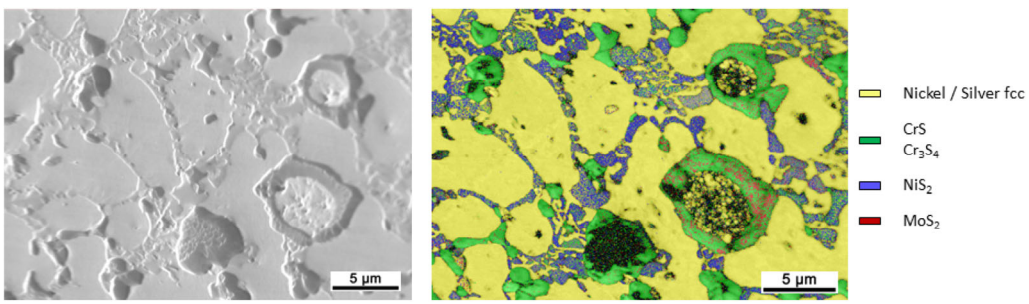

Fig. 3 Microstructure and phase distribution for the as-deposited Ni–5Ag–10MoS_2, as found by EBSD.

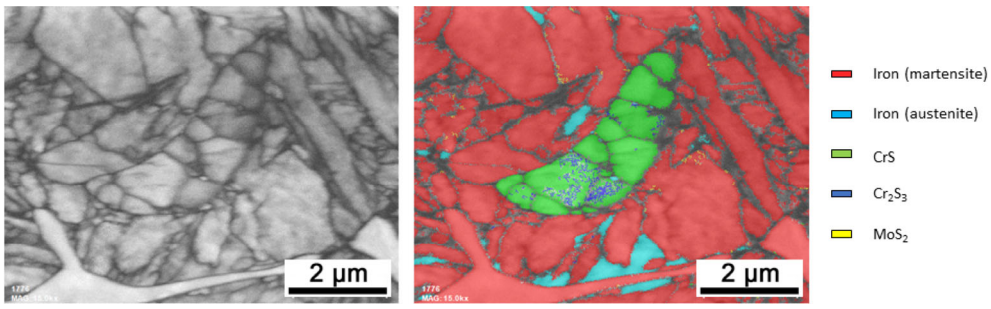

Fig. 4 Detail of the microstructure and phase distribution, as found by EBSD, for the as-deposited Fe–5Ag–10MoS_2.

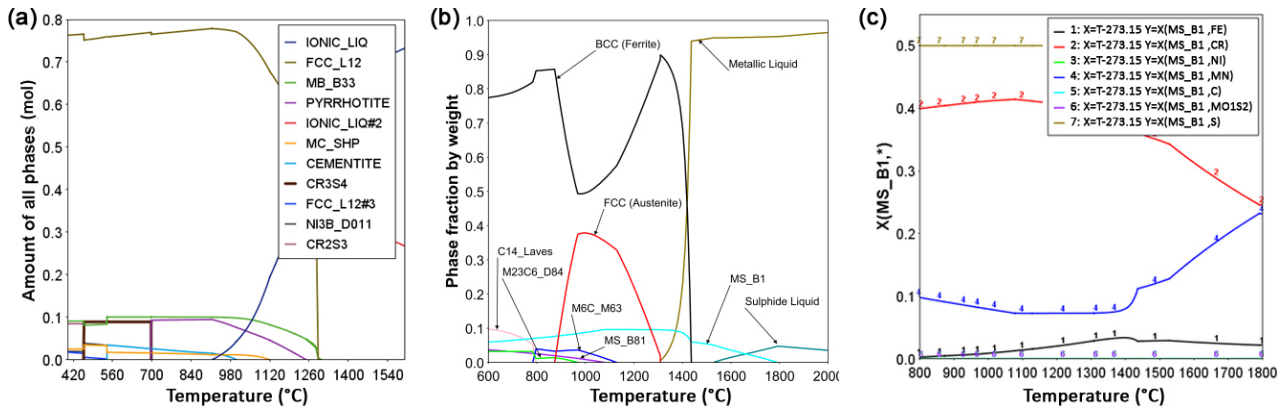

Fig. 5 Phase evolution as predicted by Thermocalc for the following systems. (a) NiCrSiB with the addition of MoS_2 and (b) FeCrNi with the addition of MoS_2 with (c) the composition of the metal sulfide MS_B1 with temperature.

In the present case, the sulfides are expected to be chromium-based.

As the remaining liquid phase cooled down, new phases were expected to form such as molybdenum carbides, which have been previously detected in similar as-deposited claddings by the authors [46]. In the context of the simulation, lower temperatures were predicted to entail a rapid phase transformation of the chromium sulfides labelled as pyrrhotite to Cr_3S_4, which is stable from 700 to ~450 °C, decomposing to Cr_2S_3 at even lower temperatures. EBSD measurements performed on the as-deposited Ni–5Ag–10 MoS_2 (Fig. 3) reported, contrarily, a combination of CrS and Cr_3S_4. This discrepancy can be explained to the fast cooling inherent to the laser cladding process, preventing the diffusional transformation of chromium sulfides to Cr_2S_3. However, it must also be noted here that the nickel sulfides detected by EBSD for Ni–5Ag–10MoS_2 could not suitably be captured by the simulations.

As for the iron-based FeCrNi–10MoS_2 system (Fig. 5(b)), two immiscible liquids were again predicted in the melt pool, as similarly seen in the iron-sulfur binary phase diagram [53]. Interestingly, the sulfur-rich liquid was predicted to start to solidify at 1,800 °C with the formation of a metallic (Mn, Cr) sulfide labelled MS_B1, with a reported NaCl structure and featuring a chromium content increasing with decreasing temperatures (see Fig. 5(c) for details). The remaining metal-rich liquid phase would subsequently solidify quickly at temperatures around 1,400 °C according to the simulation, giving rise to a dominant ferritic (bcc) matrix in addition to a minor austenitic (fcc) phase thermodynamically stable down to ~850 °C. The rapid cooling during laser cladding is responsible for the martensitic matrix and the retained austenite observed in the as-deposited iron-based cladding (Fig. 4), even though the presence of these two phases was not captured by the simulations. A carbide phase labelled as M23C6_D84, possibly $Cr_{23}C_6$, was also predicted to form below 1,000 °C while the formation of additional sulfide phases was predicted for temperatures close to 1,100 °C, labelled as MS_B81. Chromium sulfides form a compound family consisting among others of Cr_2S_3 and Cr_3S_4, non-stoichiometric on a great degree and thus difficult to quantify, with

EBSD measurements in this case favouring CrS and Cr_2S_3. In any case, both Thermocalc and EBSD results suggest significant differences for the chromium sulfide phases forming in the iron- and nickel-based self-lubricating claddings, which can determine their tribological behaviour at HT, as it will be detailed below.

3.2 High temperature reciprocating tests

The friction results for both Fe-based claddings under reciprocating sliding against AISI 52100 pins are shown in Fig. 6 for all three temperatures (RT, 400, and 600 °C). Friction results corresponding to Ni–5Ag–10MoS_2 have been included for comparison, taken from Ref. [23].

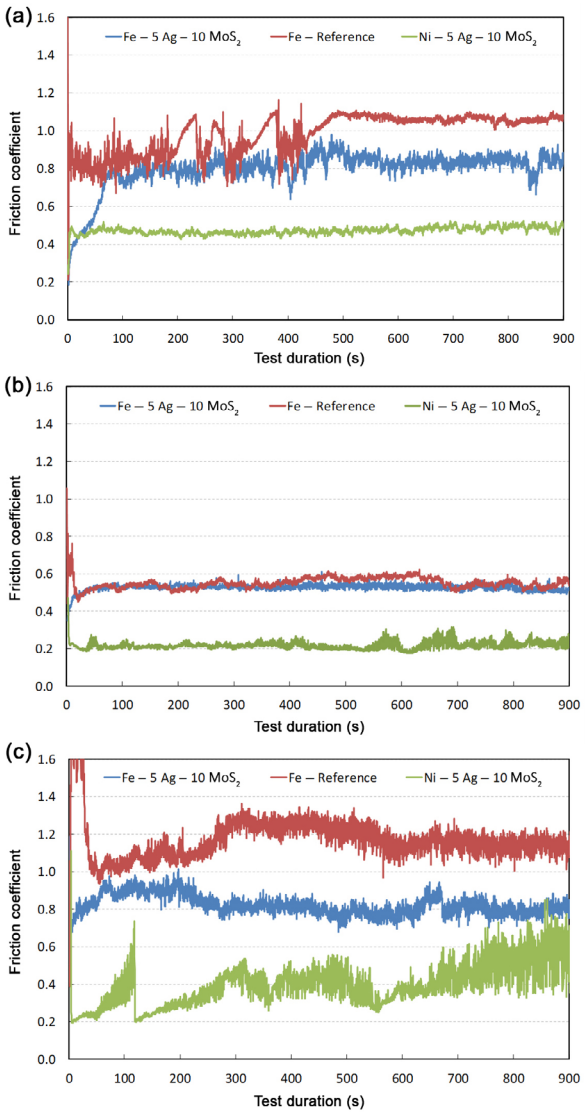

Fig. 6 Friction results against AISI 52100 at RT for Ni–5Ag–10MoS_2, Fe–5Ag–10MoS_2, and Fe-Reference at (a) RT, (b) 400 °C, and (c) 600 °C. Friction values for the nickel-based self-lubricating cladding have been taken from Ref. [23].

At RT (Fig. 6(a)), the iron-based self-lubricating cladding Fe–5Ag–10MoS_2 experienced a steadily increasing friction for the first 90 s, stabilising above 0.7 and remaining close to 0.8 for the rest of the test duration. This behaviour was considered better than that of the unmodified Fe-Reference alloy, which showed high frictional instability during the first half of the test stabilising thereafter around 1.1. However, the nickel-based self-lubricating cladding Ni–5Ag–10MoS_2 outperformed its iron-based counterpart in terms of friction, as it remained close to 0.5 for most of the test.

Increasing the temperature to 400 °C led to a more stable behaviour for both Fe-based claddings, as seen in Fig. 6(b). For the self-lubricating Fe–5Ag–10MoS_2, friction increased to 0.5 in about 60 s and remained remarkably stable afterwards. The Fe-Reference alloy on the other hand experienced a frictional peak early on up to 1.0 and with a duration close to 30 s, stabilising between 0.5 and 0.6 for the rest of the test duration. It must be noted here that such peaks have been linked with increased running-in wear in the Ref. [54]. As for the nickel-based cladding, Ni–5Ag–10MoS_2 showed a stable friction close to 0.3, again lower than the Fe-based claddings.

The maximum temperature of 600 °C led to a more unstable behaviour for all of the claddings (Fig. 6(c)). The self-lubricating Fe–5Ag–10MoS_2 experienced a friction close to 0.8 for most of the test duration, while the reference Fe-based alloy showed an extended frictional spike early on, above 1.6 and with a duration close to 60 s. Although the addition of Ag and MoS_2 did decrease friction for the Fe-based alloy, the nickel-based self-lubricating cladding Ni–5Ag–10MoS_2 experienced lower friction, although more unstable than at lower temperatures. At 600 °C, friction increased steadily from 0.2 early on to 0.7 by the end of the test, although still lower than the values observed for Fe–5Ag–10MoS_2. These results suggest that besides the addition of solid lubricants like Ag and MoS_2, some other mechanism or compound is responsible for the comparatively low friction of the nickel-based alloy.

Wear rates for the chosen claddings after reciprocating testing are plotted in Fig. 7. At RT, both self-lubricating claddings Fe–5Ag–10MoS_2 and Ni–5Ag–10MoS_2 showed comparatively low wear (2.1×10^{-5} and 2.5×10^{-5} mm³/(N·m), respectively), almost a third of the wear experienced by the Fe-Reference alloy (6.8×10^{-5} mm³/(N·m)). At 400 °C, the wear rate of the self-lubricating Fe–5Ag–10MoS_2 decreased two orders of magnitude down to 2.1×10^{-7} mm³/(N·m), while for Fe-Reference the process was more moderate, with a fivefold decrease down to 1.1×10^{-5} mm³/(N·m). As for Ni–5Ag–10MoS_2, previous testing performed at a temperature of 400 °C showed a cladding wear rate of 3.3×10^{-5} mm³/(N·m), clearly higher than for its Fe-based counterparts. At the maximum testing temperature of 600 °C, a more severe tribological behaviour could be observed: for Fe–5Ag–10MoS_2 the observed wear increased to 1.2×10^{-5} mm³/(N·m), while it significantly increased for the Fe-Reference up to 2.4 $\times10^{-4}$ mm³/(N·m), also with a significant scatter. Interestingly, the nickel-based Ni–5Ag–10MoS_2 showed a very high wear (2.4×10^{-4} mm³/(N·m)), significantly higher than its iron-based self-lubricating counterpart.

The wear rates of the AISI 52100 counter bodies after reciprocating sliding are plotted in Fig. 8. At RT, the self-lubricating Fe–5Ag–10MoS_2 more than halved the wear loss of the bearing steel counter body compared to the iron-based reference alloy (1.9×10^{-5} and 4.2×10^{-5} mm³/(N·m), respectively). Ni–5Ag–10MoS_2 led to even lower wear rates (1.2×10^{-5} mm³/(N·m)), although with a significant scatter. Increasing the

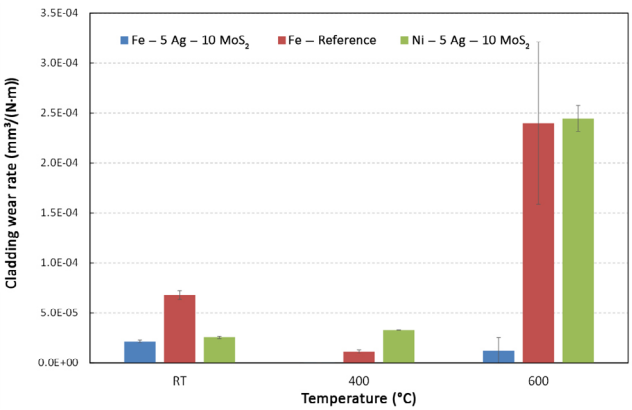

Fig. 7 Measured wear loss for the claddings after reciprocating testing against AISI 52100. Results for the Ni–5Ag–10MoS_2 cladding have been taken from Ref. [23].

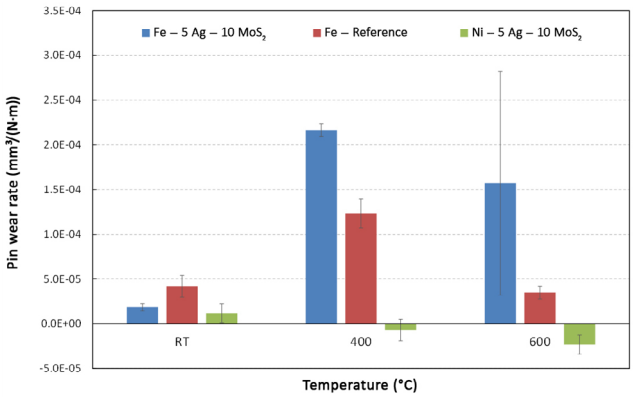

Fig. 8 Measured wear loss for the AISI 52100 pins after reciprocating testing.

testing temperature to 400 °C led to a significantly increased damage to the counter body by both Fe-based cladding: 1.2×10^{-4} mm³/(N·m) for the unmodified reference, and 2.2×10^{-4} mm³/(N·m), more than an order of magnitude higher than at RT. Interestingly, for Ni–5Ag–10MoS_2 the measured pin wear at 400 °C turned out to be negligible, in some cases even negative, suggesting material transfer from the cladding and with an average value of 7.0×10^{-6} mm³/(N·m). The maximum testing temperature of 600 °C led to qualitatively similar values: high counter body wear for the self-lubricating Fe–5Ag–10MoS_2, this time 1.6×10^{-4} mm³/(N·m) although this time with a significant scatter, and a much lower value of 3.5×10^{-5} mm³/(N·m) for the iron-based reference. The self-lubricating nickel-based was observed to outperform its Fe-based counterparts, with a clear material gain in the counter body which was able to prevent further damage to it. The underlying mechanism proved in this case to be notably effective, as low-alloyed steel grades such as AISI 52100 have been reported to significantly soften at high temperatures [39], losing mechanical strength and being susceptible to increased wear through mechanisms such as abrasion.

The wear characterisation of both Fe-based claddings and the AISI 52100 pins showed two different behaviours depending on the temperature range: at RT, both self-lubricating claddings (Fe–5Ag–10MoS_2 and Ni–5Ag–10MoS_2) led to lower cladding and counter body wear compared to the Fe-Reference alloy, which has been linked to the addition of solid lubricants like Ag and MoS_2. However, this behaviour did not take place at HT: for Fe–5Ag–10MoS_2 low

cladding wear rates could be observed at 400 and 600 °C coupled to large counter body material loss and tribolayer formation on the cladding due to wear debris compaction. The opposite was seen for the nickel-based Ni–5Ag–10MoS_2. Interestingly, the Fe-Reference alloy showed low cladding wear at 400 °C linked to high counter body wear, while the opposite could be observed at 600 °C, with no clear explanation for this behaviour. In any case, from the previous it can be inferred that at HT a mechanism exists that shifts wear between the cladding and the counter body, with no clear role of the addition of Ag and MoS_2.

In order to gain further information into the wear mechanisms affecting the tribological behaviour of the iron-based claddings, SEM/EDS characterisation was performed on the wear scars found in the coatings after testing. At RT, the Fe-Reference surface was irregularly covered with iron oxide, likely from the worn AISI 52100 counter body (spot A in Fig. 9 and Table 6). In contrast, the wear scar in Fe–5Ag–10MoS_2 showed a smoother surface (Fig. 10(a)) with visible chromium sulfide aggregates, as in the base cladding. Additionally, the smearing of silver could also be seen (Figs. 10(c) and 10(d)), suggesting effective lubrication by the soft metal. It is assumed that the decreased friction and wear of Fe–5Ag–10MoS_2 compared to Fe-Reference was due to the effective lubrication at RT by silver and the chromium sulfides forming from the thermal degradation of MoS_2, although no significant silver transfer from the cladding could be observed on the worn counter body.

The maximum testing temperature of 600 °C showed the onset of both wear damage and material transfer consisting of oxidised AISI 52100 steel to Fe–5Ag–10MoS_2 (Figs. 10(e) and 10(f), also spot B in Table 6), even if wear rates at that temperature were very different for Fe-Reference and Fe–5Ag–10MoS_2.

In order to obtain further information on the different wear rates observed for the AISI 52100 counter bodies after testing, SEM/EDS analysis was performed on worn bearing steel pins after testing at 600 °C against both self-lubricating claddings, Fe–5Ag–10MoS_2 and Ni–5Ag–10MoS_2, as shown in Fig. 11. Significant differences in the morphology and chemistry of the pin surface could be observed, even when the same solid lubricants had been incorporated to both laser claddings.

After testing against the nickel-based Ni–5Ag–10MoS_2, the surface of the AISI 52100 pin was found to be relatively smooth, with small flat patches. A similar material build-up mechanism on the counter body has been reported in the literatures for Ni-based alloys [55, 56]. Detailed EDS characterisation (Fig. 11(b) showed that the observed patches consisted mostly of transferred material from the Ni-based cladding (spot A in Table 7), with close to 75 at% of nickel but also significant sulfur (8.4 at%) and oxygen (10.3 at%)

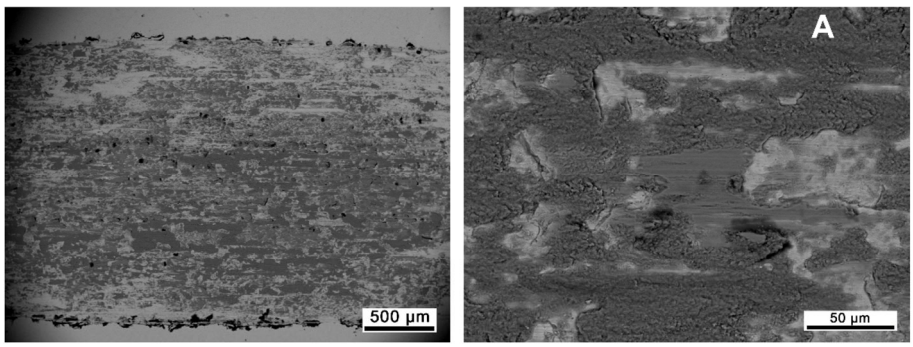

Fig. 9 SEM imaging performed on the wear scars found on Fe-Reference samples after testing at RT.

Table 6 Chemical composition as seen by EDS of the spots marked in Figs. 9 and 10.

Spot	Chemical composition (at%)							
	Fe	Ni	Mo	Cr	S	Si	Ag	O
A	74.2	—	—	3.0	—	0.5	—	22.3
B	70.3	—	—	2.7	—	—	—	26.0

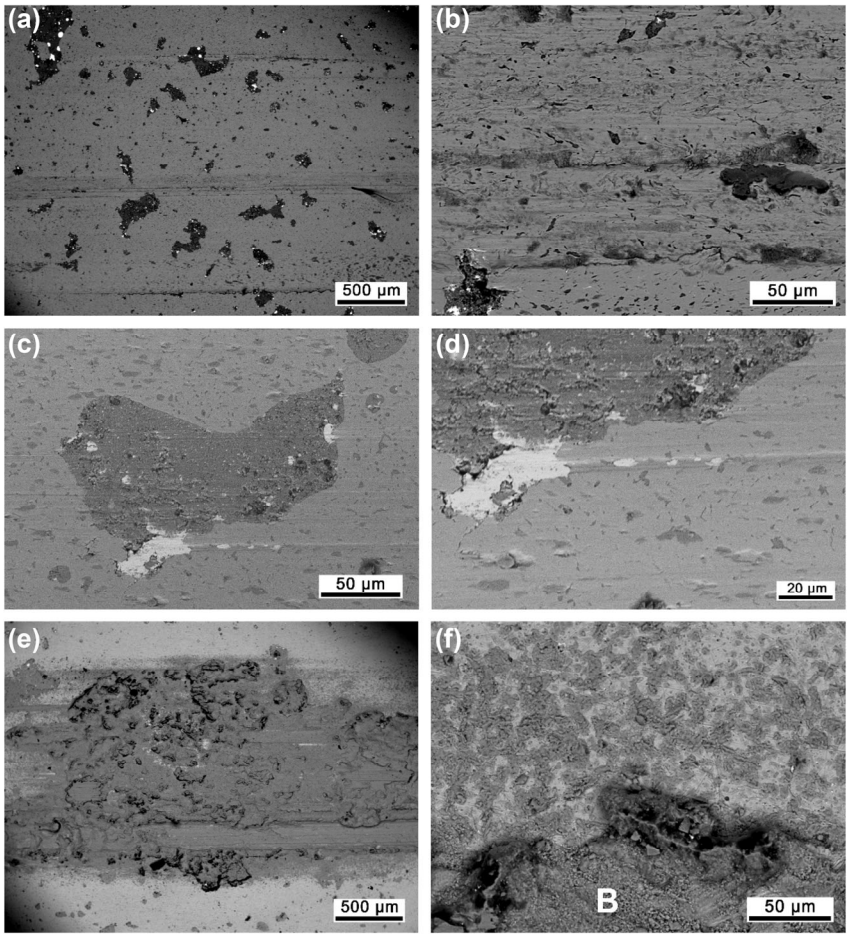

Fig. 10 SEM images performed on the wear scars found on Fe–5Ag–10MoS_2 samples after testing at (a, b) RT with a detail on (c, d) smeared silver particles and additionally at (e, f) 600 °C.

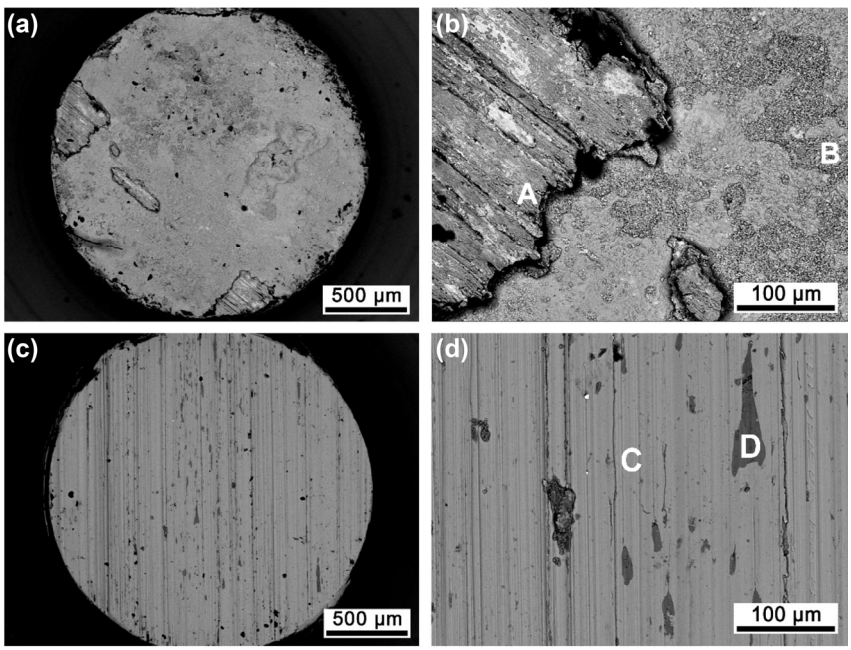

Fig. 11 SEM/EDS measurements on AISI 52100 pin after testing at 600 °C against (a, b) Ni–5Ag–10MoS_2 and (c, d) Fe–5Ag–10MoS_2.

Table 7 Chemical composition as measured by EDS of the spots marked in Fig. 11.

Spot	Chemical composition (at%)							
	Fe	Ni	Mo	Cr	S	Si	Ag	O
A	2.4	74.1	—	1.9	8.4	1.7	—	10.3
B	10.4	70.3	2.5	2.5	4.6	2.7	0.7	6.4
C	94.9	—	—	1.3	—	—	—	2.6
D	71.3	—	—	1.5	—	0.7	—	25.7

contents. Interestingly, this transferred material could also be found in the form of coarse particles covering the Fe-based substrate (spot B in Fig. 11(b) and Table 7), suggesting that it formed from the agglomeration of wear debris from the Ni-based self-lubricating cladding. A cross section performed on a worn pin after testing against the Ni-based cladding at 600 °C is given in Fig. 12, showing a discontinuous layer with a thickness smaller than 10 μm on the AISI 52100 pin surface. Chemical characterisation by means of EDS, summarised in Table 8, confirmed that the transferred layer consisted of wear debris from the Ni-based cladding, with oxygen and sulfur contents ranging between 7.1 at% and 13.8 at% (spots A and B). Silver content was also measured to be low, with no visible smeared layer linked to decreased friction.

An additional line scan performed on the observed tribolayer (Fig. 12(c)) showed increased iron content in the lower section closest to the steel counter body substrate, attributed to diffusion facilitated by the high testing temperatures.

As for the tests performed against Fe–5Ag–10MoS_2 at 600 °C, the worn pins showed abundant abrasion marks (Fig. 11(c)), which have been related to the

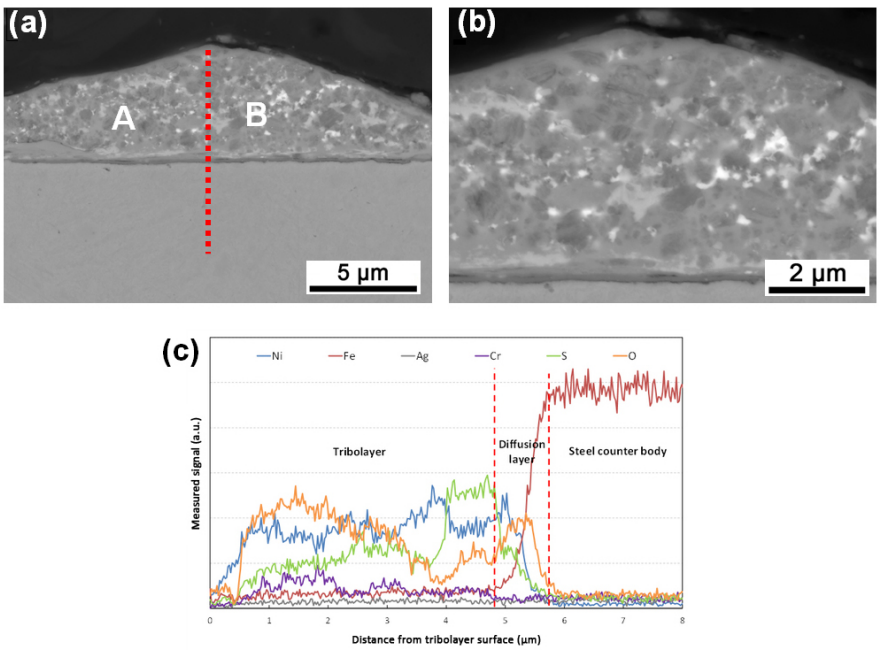

Fig. 12 (a, b) SEM/EDS measurements on a cross section of an AISI 52100 pin after testing at 600 °C against Ni–5Ag–10MoS_2. (c) Results of an additional line scan EDX measurement performed along the dashed line.

Table 8 Chemical composition as measured by EDS of the spots marked in Fig. 12.

Spot	Chemical composition (at%)							
	Fe	Ni	Mo	Cr	S	Si	Ag	O
A	5.9	41.0	3.6	2.8	13.8	2.4	0.6	28.3
B	5.6	64.9	2.2	2.8	7.1	1.4	1.2	14.2

increased material loss for the AISI 52100 pins for this series of tests. It must be reminded here that this low-alloyed steel experiences a significant softening above 500 °C [39], making it susceptible to severe abrasive wear. Chemical characterisation by means of EDS was unable to identify any tribolayer in this case. The pin surface consisted of bearing steel slightly oxidised (spot C in Fig. 11(d) and Table 7), with embedded wear debris found occasionally (spot D), although forming no protective tribolayer.

From the previous, it appears that the Ni/S/O layers forming on the counter bodies after testing against Ni–5Ag–10MoS_2 are protective in nature and lead to decreased pin wear at HT. However, no similar process could be observed for Fe–5Ag–10MoS_2, which is interesting as the same amount of solid lubricants was incorporated into the Fe-based self-lubricating claddings. Counter body characterisation thus suggests that Ni-sulfides forming on Ni–5Ag–10MoS_2 could also be potential solid lubricants, an issue which also deserves further attention. Additionally, it must also be noted here that different chromium sulfide phases were observed in the as-deposited iron- and nickel-based ones (see Table 5 for details), with Cr_3S_4 being only detected for the latter. Interestingly, this compound has been described in the available literature as an effective HT solid lubricant [57], and its crystal structure makes it possible that chromium vacancies could lead to a layered structure with easy to shear S–S bonds, not unlike those reported for TMDs [58].

In summary, during the present study both EBSD and phase diagram analysis have pointed towards significant differences for the sulfides forming in iron- and nickel-based self-lubricating claddings. This is expected to strongly influence the tribological behaviour of both self-lubricating claddings, leading to improved friction and counter body wear for the nickel-based self-lubricating cladding compared to the iron-based one. In any case, further research into the tribological behaviour of nickel- and chromium-based compounds forming at HT like oxides or sulfides is recommended.

4 Conclusions

For the present study, different iron- and nickel-based self-lubricating claddings have been systematically compared in terms of composition, microstructure, and HT tribological behaviour. In particular, the following conclusions have been reached.

1) Significant differences in terms of chemical composition and crystallographic structure have been found for the metallic sulfides forming in Ni- and Fe-based self-lubricating claddings.

2) The incorporation of the solid lubricants Ag and MoS_2 to the chosen Fe-based alloy led to decreased friction compared to the unmodified alloy, especially at RT.

3) The nickel-based self-lubricating cladding showed lower friction than its iron-based counterpart through the entire temperature range chosen for testing (RT to 600 °C).

4) In terms of cladding wear, the self-lubricating Fe–5Ag–10MoS_2 outperformed significantly the other alloys up to 600 °C.

5) The use of Fe-based claddings, regardless of solid lubricant content, led to significant counter body wear at HT, linked to material transfer of oxidised AISI 52100 steel to the claddings.

6) The differences in tribological performance between the Ni- and Fe-based self-lubricating claddings is attributed to the different composition and stoichiometry of the metal sulfides present in the cladding.

Acknowledgements

This work was funded by the Austrian COMET Programme (Project K2 InTribology, Grant No. 872176) in addition to M-ERA.NET (project 872381 HOTselflub) and has been carried out within the "Austrian Excellence Center for Tribology" (AC2T research GmbH). The authors would also like to acknowledge Tribotecc GmbH for kindly providing the MoS_2 powder used in the preparation of the self-lubricating claddings.

References

[1] De Mello J D B, Binder C, Hammes G, Binder R, Klein A N. Tribological behaviour of sintered iron based self-lubricating composites. *Friction* **5**(3): 285–307 (2017)

[2] Luo J, Zhou X. Superlubricitive engineering—Future industry nearly getting rid of wear and frictional energy consumption. *Friction* **8**(4): 643–665 (2020)

[3] Fan X Q, Xue Q J, Wang L P. Carbon-based solid–liquid lubricating coatings for space applications–A review. *Friction* **3**(3): 191–207 (2015)

[4] Huai W J, Zhang C H, Wen S Z. Graphite-based solid lubricant for high-temperature lubrication. *Friction* **9**(6): 1660–1672 (2021)

[5] Meng Y G, Xu J, Jin Z M, Parkash B, Hu Y Z. A review of recent advances in tribology. *Friction* **8**(2): 221–300 (2020)

[6] Decrozant-Triquenaux J, Pelcastre L, Prakash B, Hardell J. Influence of lubrication, tool steel composition, and topography on the high temperature tribological behaviour of aluminium. *Friction* **9**(1): 155–168 (2021)

[7] Sliney H E. Plasma-sprayed metal-glass and metal-glass fluoride coatings for lubrication to 900 °C. *ASLE Trans* **17**: 182–189 (1974)

[8] Aouadi S M, Paudel Y, Simonson W J, Ge Q, Kohli B, Muratore C, Voevodin A A. Tribological investigation of adaptive Mo_2N/MoS_2/Ag coatings with high sulfur content. *Surf Coatings Technol* **203**: 1304–1309 (2009)

[9] Muratore C, Voevodin A A, Hu J J, Zabinski J S. Tribology of adaptive nanocomposite yttria-stabilized zirconia coatings containing silver and molybdenum from 25 to 700 °C. *Wear* **261**:797–805 (2006)

[10] Khadem M, Penkov O V., Yang H K, et al. Tribology of multilayer coatings for wear reduction: A review. *Friction* **5**(3): 248–262 (2017)

[11] Wang H D, Ma G Z, Xu B S, Yong Q S, He P F. Design and application of friction pair surface modification coating for remanufacturing. *Friction* **5**(3): 351–360 (2017)

[12] Chen J, An Y, Yang J, Zhao X Q, Yan F Y, Zhou H D, Chen J M. Tribological properties of adaptive NiCrAlY–Ag–Mo coatings prepared by atmospheric plasma spraying. *Surf Coatings Technol* **235**: 521–528 (2013)

[13] Ouyang J H, Li Y F, Wang Y M, Zhou Y, Murakami T, Sasaki S. Microstructure and tribological properties of $ZrO_2(Y_2O_3)$ matrix composites doped with different solid lubricants from room temperature to 800 °C. *Wear* **267**: 1353–1360 (2009)

[14] Kong L, Bi Q, Niu M, et al. ZrO_2 (Y_2O_3)–MoS_2–CaF_2 self-lubricating composite coupled with different ceramics from 20 °C to 1000 °C. *Tribol Int* **64**: 53–62 (2013)

[15] Zhen J M, Cheng J, Tan H, Sun Q C, Zhu S Y, Yang J, Liu W M. Investigation of tribological characteristics of nickel alloy-based solid-lubricating composites at elevated temperatures under vacuum. *Friction* **9**(5): 990–1001 (2021)

[16] Kang X, Yu S, Yang H L, Sun Y, Zhang L. Tribological behavior and microstructural evolution of lubricating film of silver matrix self-lubricating nanocomposite. *Friction* **9**(5): 941–951(2021)

[17] Garrido A H, González R, Cadenas M, HernándezBattez A. Tribological behavior of laser-textured NiCrBSi coatings. *Wear* **271**: 925–933 (2011)

[18] Fernández M R, García A, Cuetos J M, González R, Noriega A, Cadenas M. Effect of actual WC content on the reciprocating wear of a laser cladding NiCrBSi alloy reinforced with WC. *Wear* **324**: 80–89 (2015)

[19] Riveiro A, Mejías A, Lusquiños F, del Val J, Comesaña R, Pardo J, Pou J. Laser cladding of aluminium on AISI 304 stainless steel with high-power diode lasers. *Surf Coatings Technol* **253**: 214–220 (2014)

[20] Information. https://web.archive.org/web/*/www.lcc.fi/pdf/Process_basics_and_coating_properties.pdf , 2017.

[21] Dubourg L, Archambeault J. Technological and scientific landscape of laser cladding process in 2007. *Surf Coatings Technol* **202**: 5863–5869 (2008)

[22] Toyserkani E, Khajepour A, Corbin S. Laser cladding equipment. In *Laser Cladding*. Boca Raton: CRC Press LLC, 2005: 41–80.

[23] Torres H, Vuchkov T, Slawik S, Gachot C, Prakash B, Rodríguez Ripoll M. Self-lubricating laser claddings for reducing friction and wear from room temperature to 600 °C. *Wear* **408–409**: 22–33 (2018)

[24] Torres H, Slawik S, Gachot C, Prakash B, Rodríguez Ripoll M. Microstructural design of self-lubricating laser claddings for use in high temperature sliding applications. *Surf Coatings Technol* **337**: 24–34 (2018)

[25] Niu W, Sun R, Lei Y. Microstructure and wear properties of laser clad NiCrBSi–MoS_2 coating. *Frict Wear Res* **2**: 1–5 (2014)

[26] Yang M S, Liu X B, Fan J W, et al. Microstructure and wear behaviors of laser clad NiCr/Cr_3C_2–WS_2 high temperature self-lubricating wear-resistant composite coating. *Appl Surf Sci* **258**: 3757–3762 (2012)

[27] Yan H, Zhang J, Zhang P L, Yu Z S, Li C G, Xu P Q, Lu Y L. Laser cladding of Co-based alloy/TiC/CaF_2 self-lubricating composite coatings on copper for continuous casting mold. *Surf Coatings Technol* **232**: 362–369 (2013)

[28] Xu J, Liu W, Zhong M. Microstructure and dry sliding wear behavior of MoS_2/TiC/Ni composite coatings prepared by laser cladding. *Surf Coatings Technol* **200**: 4227–4232 (2006)

[29] Arias-González F, del Val J, Comesaña R, Penide J, Lusquiños F, Quintero F, Riveiro A, Boutinguiza M, Pou J. Fiber laser cladding of nickel-based alloy on cast iron. *Appl Surf Sci*. **374**: 197–205 (2016)

[30] Kumar V, Kumar S, Anand M, Kumar V, Das A K. Fiber Laser Cladding of WS_2 + Cr on SS316 Substrate and its Characterization. *Mater Today Proc* **22**: 1645–1651 (2019)

[31] Piasecki A, Kotkowiak M, Kulka M. Self-lubricating surface layers produced using laser alloying of bearing steel. *Wear* **376–377**: 993–1008 (2017)

[32] OuYang C S, Liu X B, Luo Y S, Liang J, Wang M, Chen D Q. Preparation and high temperature tribological properties of laser *in-situ* synthesized self-lubricating composite coating on 304 stainless steel. *J Mater Res Technol* **9**: 7034–7046 (2020)

[33] Awasthi R, Limaye P K, Kumar S, Kushwaha R P, Viswanadham C S，Srivastava D，Soni N L，Patel R J, Dey G K. Wear characteristics of Ni-based hardfacing alloy deposited on stainless steel substrate by laser cladding. *Metall Mater Trans A Phys Metall Mater Sci* **46**:1237–1252 (2015)

[34] Jin L, Edrisy A, Riahi AR. Analysis of Ti–6Al–4V adhesion to AISI 52100 steel and TiN during unlubricated sliding contact. *Tribol Int* **90**: 278–286 (2015)

[35] Li J L, Xiong D S. Tribological properties of nickel-based self-lubricating composite at elevated temperature and counterface material selection. *Wear* **265**: 533–539 (2008)

[36] Lin F H, Xia Y Q, Feng X. Conductive and tribological properties of TiN–Ag composite coatings under grease lubrication. *Friction* **9**(4): 774–788 (2021)

[37] Xiao J K, Wu Y Q, Zhang W, Chen J, Zhang C. Friction of metal-matrix self-lubricating composites: Rrelationships among lubricant content, lubricating film coverage, and friction coefficient. *Friction* **8**(3): 517–530 (2020)

[38] Zhang Y P, Li P P, Ji L, Liu X H, Wan H Q, Chen L, Li H X, Jin Z L. Tribological properties of MoS_2 coating for ultra-long wear-life and low coefficient of friction combined with additive g-C_3N_4 in air. *Friction* **9**(4): 789–801 (2021)

[39] Torres H, Varga M, Rodríguez Ripoll M. High temperature hardness of steels and iron-based alloys. *Mater Sci Eng A* **671**: 170–181 (2016)

[40] Ghiotti A, Bruschi S, Borsetto F. Tribological characteristics of high strength steel sheets under hot stamping conditions. *J Mater Process Technol* **211**: 1694–1700 (2011)

[41] Yanagida A, Azushima A. Evaluation of coefficients of friction in hot stamping by hot flat drawing test. *CIRP Ann-Manuf Technol* **58**: 247–250 (2009)

[42] Pelcastre L, Hardell J, Prakash B. Galling mechanisms during interaction of tool steel and Al–Si coated ultra-high strength steel at elevated temperature. *Tribol Int* **67**: 263–271 (2013)

[43] Cora ÖN, Ağcayazı A, Namiki K, Sofuoğlu H, Koç M. Die wear in stamping of advanced high strength steels—Investigations on the effects of substrate material and hard-coatings. *Tribol Int* **52**: 50–60 (2012)

[44] Dohda K, Yamamoto M, Hu C L, Dubar L, Ehmann K F. Galling phenomena in metal forming. *Friction* **9**(4): 665–685 (2021)

[45] Venema J, Hazrati J, Atzema E, Matthews D, van den Boogaard T. Multiscale friction model for hot sheet metal forming. *Friction* 10(2): 316–334 (2022)

[46] Torres H, Vuchkov T, Ripoll M R, Prakash B. Tribological behaviour of MoS_2-based self-lubricating laser cladding for use in high temperature applications. *Tribol Int* **126**: 153–165 (2018)

[47] Tomoshige R, Niitsu K, Sekiguchi T, Oikawa K, Ishida K. Some tribological properties of SHS-produced chromium sulfide. *Int J Self-Propagating High-Temperature Synth* **18**: 287–292 (2009)

[48] Torres H, Caykara T, Rojacz H, et al. The tribology of Ag / MoS_2-based self-lubricating laser claddings for high temperature forming of aluminium alloys. *Wear* **442–443**: 203110 (2020)

[49] Torres H, Rodríguez R M, Prakash B. Self-lubricating laser claddings for friction control during press hardening of Al–Si-coated boron steel. *J Mater Process Technol* **269**: 79–90 (2019)

[50] Yadav P, Lee D B. Corrosion of Inconel 690 in N_2–0.1%H_2S gas at 700–800 °C. *Met Mater Int* **23**: 893–899 (2017)

[51] ASM International Handbook Committee. Ni (Nickel) Binary Alloy Phase Diagrams. In *ASM Metals Handbook Volume 3: Alloy Phase Diagrams*. Baker H, Ed. Materials Park: ASM International, 1992: 1212–1250.

[52] Lei Y, Sun R, Tang Y, Niu W. Microstructure and phase transformations in laser clad Cr_xS_y/Ni coating on H13 steel. *Opt Lasers Eng* **66**: 181–186 (2015)

[53] ASM International Handbook Committee. Fe (Iron) Binary Alloy Phase Diagrams. In *ASM Metals Handbook Volume 3: Alloy Phase Diagrams*. Baker H, Ed. Materials Park: ASM International, 1992: 826–877.

[54] Torres H, Varga M, Adam K, Rodríguez Ripoll M. The role of load on wear mechanisms in high temperature sliding contacts. *Wear* **364–365**: 73–83 (2016)

[55] Tudela I, Cobley A J, Zhang Y. Tribological performance of novel nickel-based composite coatings with lubricant particles. *Friction* **7**(2): 169–180 (2019)

[56] Bai L Y, Wan S H, Yi G W, Shan Y, The Pham S, Tieu A K, Li Y, Wang R D. Temperature-mediated tribological characteristics of 40CrNiMoA steel and Inconel 718 alloy during sliding against Si_3N_4 counterparts. *Friction* **9**(5): 1175–1197 (2021)

[57] Li J L, Xiong D S, Huo M F. Friction and wear properties of Ni–Cr–W–Al–Ti–MoS_2 at elevated temperatures and self-consumption phenomena. *Wear* **265**: 566–575 (2008)

[58] Colgan D C, Powell A V. A combined time-of-flight powder neutron and powder X-ray diffraction study of ternary chromium sulfides $V_xCr_{3-x}S_4$ ($0 < x < 1.0$). *J Mater Chem* **6**:1579–1584 (1996)

Hector TORRES. He holds a B.Sc. degree in physics and works at the Austrian Excellence Center for Tribology since 2012. In 2019 he received his Ph.D. degree from Luleå University of Technology. His main research topics include high temperature tribology, friction, and self-lubricating materials prepared by means of laser cladding.

Tugce CAYKARA. She holds a Tribos-Joint European master degree in tribology of surfaces and interfaces and a bachelor in science with a major in chemical engineering from Istanbul University. She has conducted her doctoral studies at the University of Minho in modification of polymer surfaces to render antibacterial properties. Her research interests include soft and hard matter tribology in addition to antiadhesive multifunctional surfaces.

Jens HARDELL. He obtained his M.Sc. degree in mechanical engineering in 2005 from Luleå University of Technology. In 2009, he completed his Ph.D. in machine elements at Luleå University of Technology. He became associate professor at the Division of Machine Elements, Luleå University of Technology, in 2014 as well as head of Division in 2016 and full professor at the Division of Machine Elements in 2021. He has been a visiting professor at Université de Lyon, Ecole Nationale d'Ingénieurs de Saint-Etienne in France. His main research and teaching interests include high temperature tribology, friction and wear in dry contacts, tribomaterials, surface engineering for friction and wear control, wear and failure analysis, and machine components.

Janne NURMINEN. He holds a Ph.D. on laser cladding and has been working for research and development in materials science for more than 20 years. He has about 10 published peer-reviewed papers, with most of his work being done for the industry. His research interests include welding, coatings, wear, corrosion, and hot isostatic pressing. Currently he works for Castolin Eutectic in Switzerland.

Braham PRAKASH. He obtained his BSc Eng (mechanical) degree from Punjab Engineering College, Chandigarh (India), and M Tech (mechanical engineering) as well as Ph.D. (tribology) degrees from Indian Institute of Technology Delhi (India). He is a professor emeritus at the Division of Machine Elements of Luleå University of Technology in Sweden since 2019 and a distinguished visiting professor at the Department of Mechanical Engineering of Tsinghua University in China since 2018. He has earlier been professor and head of Tribolab at the Division of Machine Elements of Luleå University of Technology from 2002 to 2019. He has also been a faculty member at Indian Institute of Technology Delhi from 1981 to 2002, a visiting professor at Tokyo University of Science, Japan (2016) and Indian Institute of Technology, Ropar, India (2010–2013), Japan Society for the Promotion of Science (JSPS) postdoctoral fellow, Chiba Institute of Technology, Japan (1998–2000) and visiting researcher at Tokyo Institute of Technology, Japan (1985).

Professor Prakash has over 45 years of experience, both in academia and industry. His research and teaching activities cover several aspects of tribology such as high temperature tribology, friction and wear of materials, solid and boundary lubrication, surface engineering, tribology of machine components, tribology of wheel-rail interface, tribotesting, and analysis and solution of tribological problems. He has mentored over 10 postdoc researchers, 18 Ph.D. candidates, and numerous students. He has made over 250 contributions in reputed journals, international conferences, and books.

Manel RODRÍGUEZ RIPOLL. He leads the research area "Wear Reduction Strategies for Industry" at the Austrian Excellence Center for Tribology. His main research focuses on surface engineering for reducing wear in extreme environments. Current topics of research are the design of self-lubricating materials, surface protection in tribocorrosive environments for offshore and biomedical applications and the tribochemical formation of two-dimensional solid lubricants. He graduated in physics in Barcelona, Spain and holds a Ph.D. in mechanical engineering from the Karlsruhe Institute of Technology, Germany. He has published over 80 peer-reviewed articles, one book, one book chapter, and three patents.